3'-Aminofluorene-9-spiro-5'-imidazolidine-2',4'-dithione as a Sensing Material for Planar Aromatic Solvents

Tomomi Sakata, Mitsuaki Suzuki

Department of Chemistry, Josai University, Sakado, 350 0198, Saitama, Japan

ABSTRACT

Herein, we investigate the non-covalent interactions between aromatic compounds and a spirocycle-bearing imidazolidinedithione molecule 3′-aminofluorene-9-spiro-5′-imidazolidine-2′,4′-dithione Host Material (**HM**). **HM** and planar aromatic solvent molecules, such as benzene, pyrrole, and thiophene, form molecular compounds with a composition ratio of 2:1 through NH···π interactions. These compounds exhibit weak emission in the λ_{max} range of 515–544 nm, which were estimated from the sum of the squares of the differences between the electronegativities of the bonded atoms comprising the guest molecule structures without employing quantum calculations. Moreover, a linear correlation between the desorption temperature and NH···π interactions is determined from the heats of formation of HM, guest molecules, and corresponding molecular compounds.

Key words: 3′-aminofluorene-9-spiro-5′-imidazolidine-2′,4′-dithione, Molecular compound, N-H···π interaction, Planar aromatic solvent.

1. INTRODUCTION

Macrocyclic hosts, such as crown ethers, calixarenes, cyclodextrins, cucurbiturils, and pillararenes, have enabled unparalleled advancements in disease diagnosis and therapy in recent years based on the principle of host-guest molecular recognition [1]. Molecular recognition refers to specific interactions between two or more molecules that occur through non-covalent bonding. Such interactions include cation–π, anion–π, π–π, and CH···π interactions, as well as hydrogen bonding, electrostatic interactions, and coordinative metal–ligand bonding; all of these interactions are frequently employed in the programmed synthesis of supermolecules and in decreasing specific van der Waals, dispersion-driven, and hydrophobic forces [2]. Supramolecular chemistry, which is based on these intermolecular interactions, involves the study of supramolecular self-assembly observed in vital components of numerous biological systems and processes, such as in nucleic acids, phospholipid membranes, proteins, ribosomes, and microtubules [3-6]. A fundamental feature of supramolecular chemistry is the investigation of the dynamic nature of non-covalent interactions and selective host–guest complexation, which give rise to molecular compounds with great potential toward the development of drug delivery systems. We have previously reported a novel non-covalent NH···π interaction that was discovered serendipitously during the synthesis of imidazolidine-2-thione derivatives as acyclic host molecules [7]. Such a compound has been known to exhibit various pharmacological and biological activities, including antimicrobial, anti-fungal, antithyroid, antioxidant, cardiotonic, anti-hypertensive, dopamine beta-hydroxylase inhibitory, and anti-HIV properties [8]. More importantly, we have previously established that one of the chemical derivatives known as 3′-aminofluorene-9-spiro-5′-imidazolidine-2′,4′-dithione Host Material (**HM**) acted as a **HM**; that is, **HM** and benzene have undergone two non-covalent intermolecular NH···π interactions to form a molecular compound (**MC1**) in a ratio of 2:1. The amino terminus of **HM** served as an "arm" that held the benzene guest molecule through non-covalent intermolecular bonding. This behavior of **HM** makes it suitable for molecular tweezing applications [9-12]. In this study, we investigated the chemical and structural aspects of planar aromatic guest molecules other than benzene that form molecular compounds with **HM** through NH···π interactions. Furthermore, we evaluated the changes in the optical-properties caused by the formation of these molecular compounds as well as the corresponding thermal characteristics of each.

2. EXPERIMENTAL

Nuclear Magnetic Resonance (NMR) spectroscopy was conducted on a Varian 400-MR spectrometer at 400 MHz. Fourier-transform infrared (FT-IR) spectra were obtained using a JASCO IR-5300 spectrometer. The emission spectra of all synthesized molecular compounds (around 100 mg) and the corresponding guest solvents (3 mL) were measured using a JASCO FP-6200 spectrofluorometer at room temperature. Crystallographic characteristics were analyzed using a single-crystal X-ray diffractometer (Bruker D8 Venture) at 90 K. Thermogravimetry-differential thermal analysis (TG-DTA) was performed using a Rigaku Thermo Plus 2 at a heating rate of 10°C/min.

2.1. HM

3′-Aminofluorene-9-spiro-5′-imidazolidine-2′,4′-dithione, whose structure is shown in Scheme 1 was prepared according to the protocol outlined in our previous work [7].

2.2. Reaction of HM with Aromatic Compounds

After HM was dissolved in a guest solvent, such as a halogenated benzene (fluorobenzene, chlorobenzene, bromobenzene), an alkyl-substituted benzene (toluene, *p*-xylene), or thiophene, a low-solubility solvent was added to precipitate the crystals. In cases wherein the guest solvent could not be used due to the immiscibility of the low-solubility HM and guest (e.g., pyrrole) solvents, the slow evaporation method was applied. This technique concentrates the solvent under reduced pressure, thereby vaporizing it until only the crystal is left. The obtained crystals were then dried under reduced pressure. For molecular compounds such as those involving naphthalene that are solid at room temperature, neither of the two methods was applicable. Hence, the crystallization of molecular compounds with this type of guest molecule was not investigated in this study.

When planar aromatic compounds pyrrole and thiophene were used as guest molecules, the IR absorption spectra of the resulting crystalline materials showed peaks at 3448 and 1045 cm^{-1}, respectively, which were not present in the IR spectrum of pure **HM**. These absorption bands correspond to the N–H and C–S stretching vibrations of pyrrole and thiophene, respectively, indicating the incorporation of the guest molecules in the microcrystalline material. ^{1}H NMR spectra confirmed that the precipitated crystals contained HM and the guest molecules in a ratio of 2:1. When halogenated benzenes with reduced π-electron density or non-planar alkyl-substituted benzenes were used as guest molecules, the IR spectra of the crystal products did not contain peaks corresponding to either halogenated or alkyl-substituted benzenes. This indicates that HM does not form the corresponding molecular compounds if the aromatic guest molecule has reduced π-electron density or is sterically hindered, as in the case of alkyl-substituted aromatics.

2.3. Preparation of Molecular Compounds Comprising HM and Planar Aromatic Solvents

Three HM–containing molecular compounds were synthesized. Firstly, HM was dissolved in benzene and evaporated under reduced pressure. The resulting residue was then recrystallized by adding 1:1 benzene/pentane. The crystals were subsequently dried at 70°C under a reduced pressure of 666 Pa for over 7.0 h to yield MC1 [7]. Next, HM was dissolved in pyrrole and was then subjected to the slow evaporation method. The obtained crystals were dried at 70°C and at a pressure of 500 Pa for 4.0 h to produce **MC2**. Finally, **HM** was dissolved in thiophene, which was then evaporated under reduced pressure. The resulting residue was recrystallized by adding *n*-hexane. The crystalline products were then dried at 70°C and at a pressure of 500 Pa for 4.0 h. The product was labeled as **MC3**. (See Supplementary Data)

3. OPTICAL PROPERTIES

On UV irradiation (λ = 365 nm), **MC1**, composed of **HM** and benzene, exhibited a weak blue-green emission, as shown in Figure 1.

The λ_{max} of pure HM was at 503 nm, while the broad signal at 515 nm indicated light emission from HM in MC1. Moreover, the λ_{max} corresponding to the π–π* transition of the guest molecule benzene
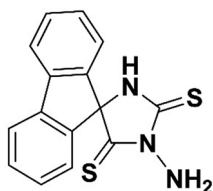
Scheme 1: Formula of chemical structure HM.

shifted from 389 to 379 nm. This shift to a shorter wavelength was attributed to the potential interaction between N–H of the amino group of HM and a π orbital of benzene (NH···π) as a result of MC1 formation [7].

In contrast, pyrrole-containing MC2 and thiophene-containing MC3 exhibited weak yellow and blue-green emissions, respectively, at λ = 365 nm. The emission spectra of MC2 and MC3 crystals as well as those of the corresponding guest solvents of each product are shown in Figure 2.

The λ_{max} at 544 and 517 nm in Figures 2(a) and 2(b) indicates the presence of HM in MC2 and MC3, respectively. In addition, the

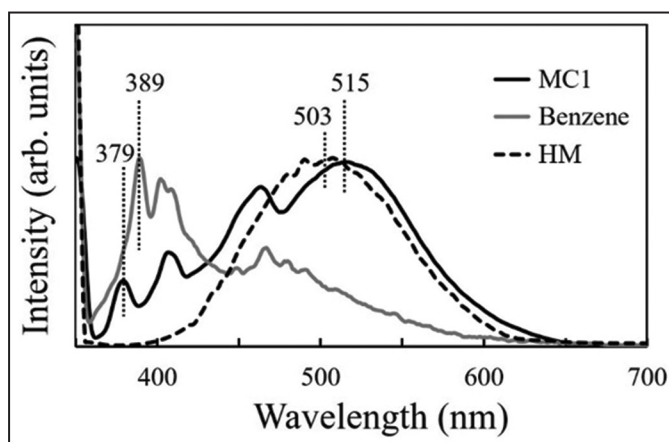**Figure 1:** Emission spectra of MC1 crystals, the benzene guest molecule, and HM at an excitation wavelength of 350 nm.
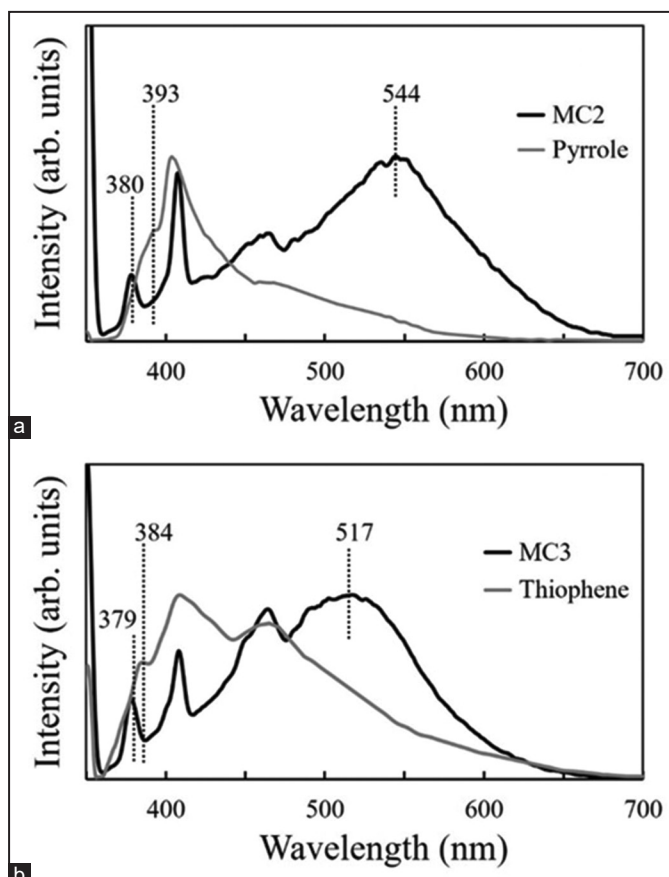
Figure 2: Emission spectra of (a) crystalline MC2 and the pyrrole guest molecule, and (b) crystalline MC3 and the thiophene guest molecule.

shifts in λ_{max} from 393 to 380 nm in Figure 2a and 384 to 379 nm in Figure 2b are ascribed to the π–π* transitions of the guest molecules within MC2 and MC3, respectively. Similar to what was established with MC1, these findings suggest the existence of NH⋯π that arise from the interactions between N–H of the amino group of HM and the π orbitals of the guest molecules.

To confirm the formation and to determine the structures of MC2 and MC3, single-crystal X-ray crystallography was performed. The obtained crystal parameters are listed in Table 1 [13-15].

As shown in Figure 3, all guest molecules are partially sandwiched between the imidazolidine rings along the c axis. However, a disorder with an occupancy ratio of 0.5:0.5 is observed in each of the two orientation directions. The structures in Figure 3 also reveal that one of the hydrogen atoms of the amino group is directed toward the ring centers of benzene (NH⋯π distances = 3.200 Å), pyrrole (NH⋯π distances = 3.197 Å), and thiophene (NH⋯π distances = 3.257 Å). This suggests that a hydrogen bond was formed through the π orbital rather than through the non-bonding orbital. Therefore, MC1, MC2, and MC3 are stabilized by two intramolecular NH⋯π interactions between HM and the guest molecules.

4. RESULTS AND DISCUSSION

The λ_{max} of **HM** at 503 nm (Figure 1) shifted to a longer wavelength on the formation of the molecular compounds. For instance, the λ_{max} values of benzene-containing **MC1** and thiophene-containing **MC3** were nearly identical at 515 and 517 nm, respectively. On the other hand, the λ_{max} for pyrrole-containing **MC2** shifted considerably to 544 nm. The highest occupied molecular orbital (HOMO) and lowest unoccupied molecular orbital (LUMO) energy levels of each molecular compound were calculated using PM5 of MOPAC (Fujitsu MOPAC 2002 Version 2.20 CACheTM); the results are shown in Figure 4.

Table 1: X-ray crystallographic parameters for the molecular compounds of interest

Moiety formula	$C_{15}H_{11}N_3S_2$, $0.5(C_6H_6)$ (MC1)	$C_{15}H_{11}N_3S_2$, $0.5(C_4H_5N)$ (MC2)	$C_{15}H_{11}N_3S_2$, $0.5(C_4H_4S)$ (MC3)
Formula weight	330.93	330.93	339.46
Crystal color	colorless	colorless	colorless
Crystal system	monoclinic	monoclinic	monoclinic
Space group	P2$_1$/c	P2$_1$/c	P2$_1$/c
a, b, c (Å)	11.1528(4), 10.1416(4), 14.4342(6)	11.0544(5), 10.0588(5), 14.4399(7)	11.1330(5), 10.0791(4), 14.4690(7)
α, β, γ (deg)	90, 103.118(1), 90	90, 103.838(2), 90	90, 103.897(2), 90
V (Å3)	1590.01(11)	1559.03 (13)	1576.05 (12)
Density (g/cm^3)	1.406	1.410	1.431
Z	4	4	4
R (ref)	0.0799 (2452)	0.0669 (2595)	0.0664 (3103)
wR2 (ref)	0.1569 (3078)	0.2048 (3356)	0.1424 (4374)
S	1.154	1.047	1.077

The LUMOs of the compounds were assigned to the π* orbital of HM, with all energy levels being approximately −1.35 eV. In contrast, the HOMO energy levels of MC1 and MC3, which were associated with the π orbital of HM, were approximately −9.03 and −9.05 eV, respectively. These values were comparable to the HOMO energy levels of pure HM at −9.06 eV. Evidently, the guest molecules had negligible influence on the HOMO energy levels of the resulting molecular compounds. For instance, the HOMO energy
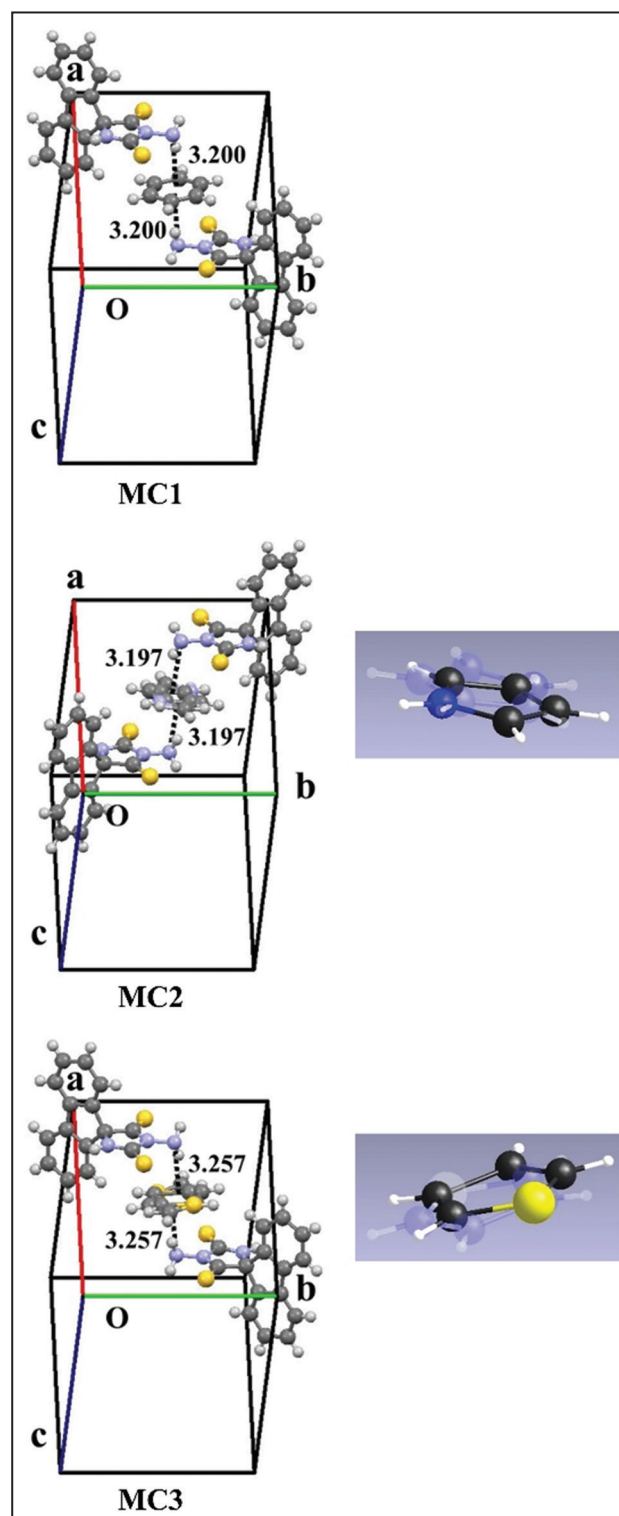
Figure 3: (Color online) Crystal structures of MC1, MC2 with disordered pyrrole, and MC3 with disordered thiophene.
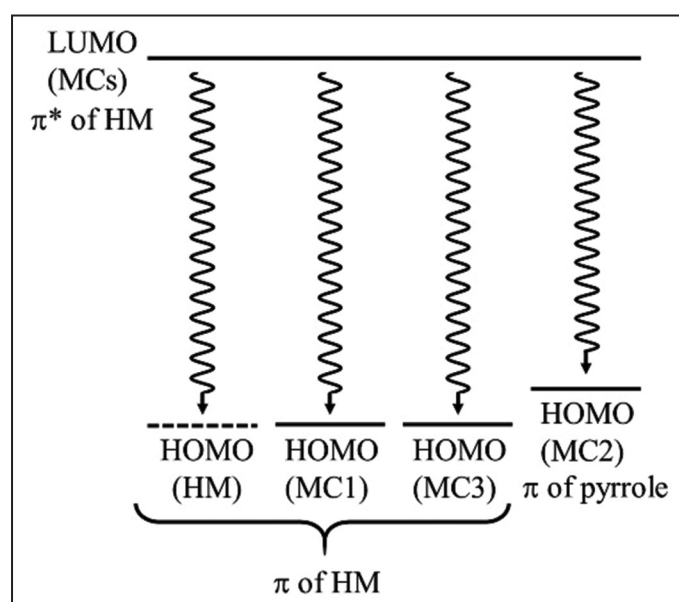
level of MC2, assigned to the π orbital of pyrrole, was at −8.86 eV. Based on these data, it was determined that the luminescence of MC1 and MC3 originates from the $\pi–\pi^*$ transition of HM, while the emission of MC2 indicates charge transfer (CT) from the guest pyrrole to HM.

The differences between the λ_{max} of HM in the molecular compounds (MC1, MC2, and MC3) and that of pure HM were 12, 41, and 14 nm, respectively. The λ_{max} of MC1 was similar to that of MC3, but markedly different from that of MC2. This was correlated with the degrees of aromaticity of the guest molecules. Aromaticity is known to be associated with resonance energy, the root square of which corresponds to the difference in electronegativity [16]. To explain the λ_{max} shift of HM in the molecular compounds, the following two relationships were investigated using the shift in reciprocal λ_{max} ($\Delta 1/\lambda_{max}$). The said parameter was taken to be the difference between the reciprocal λ_{max} of the molecular compounds and that of pure HM.

First, we studied the relationship between $\Delta 1/\lambda_{max}$ and the sum of the squares of the differences between the electronegativities of the bonded atoms present in the guest molecule structure, as shown in Eq. (1):

$$" 1 / \lambda \max = \sum_{i \neq j} (en_i - en_j)^2 \qquad (1)$$

where en_i represents the electronegativity of atom i, while subscripts i and j denote adjacent and bonded atoms. The electronegativity values used herein were those proposed by Sanderson [17,18]. Second, we attempted to correlate $\Delta 1/\lambda_{max}$ to the difference between the LUMO and HOMO energy levels of the molecular compounds. As shown in Figure 5, both relationships were linear, suggesting that the value of λ_{max}, even for unknown molecular compounds, could be simply estimated from the electronegativities of the bonded atoms comprising the guest molecule structure. Quantum calculations were not required because the LUMO energy levels of the molecular compounds were comparable. In addition, it is possible to identify the molecular compounds involved using the relationship established above, regardless of whether the observed luminescence is derived from the CT or $\pi–\pi^*$ states.

HM, a spiro 3-aminoimidazolidine-2,4-dithione derivative, is a promising host molecule with high selectivity for planar aromatic compounds as guest molecules. All λ_{max} values of HM in the molecular compounds were found to be shifted to longer wavelengths compared to those of free HM. In addition, the λ_{max} shift arising from HM can be estimated from the electronegativities of the bonded atoms comprising the guest molecule structures. Hence, HM can potentially be applied as molecular tweezers, enabling the identification of trapped molecules through emission spectroscopy following guest molecule trapping.

TG-DTA was performed to investigate the desorption temperatures of guest molecules from MC1, MC2, and MC3. From the endothermic peak in the DTA profile and the mass reduction curve in the TG profile, the desorption temperatures were determined to be at 128, 117, and 110°C for MC1, MC2, and MC3, respectively, as shown in Figure 6.

Furthermore, we examined the relationship between the desorption temperature and the NH⋯π interaction energy, as defined by Eq. (2):

$$\text{NH} \pi \text{ interaction energy}$$
$$= \frac{\left\{ 2 \times \left(\Delta H_f \text{ of } \mathbf{HM} \right) - \left(\Delta H_f \text{ of } \mathbf{GM} \right) \right\} - \left(\Delta H_f \text{ of } \mathbf{MC} \right)}{2} \qquad (2)$$

where ΔH_f is the heat of formation calculated by PM5.

From Figure 7, it is evident that the NH⋯π interaction between **HM** and benzene is the strongest while the one with thiophene as the guest molecule is the weakest. A linear correlation between the NH⋯π interaction energy and desorption temperature is also observed, suggesting that a higher NH⋯π interaction energy leads to a higher desorption temperature. In addition, the NH⋯π interaction energy for all molecular compounds was less than 15 kJ/mol, which is less than or equal to that of representative hydrogen bonds.

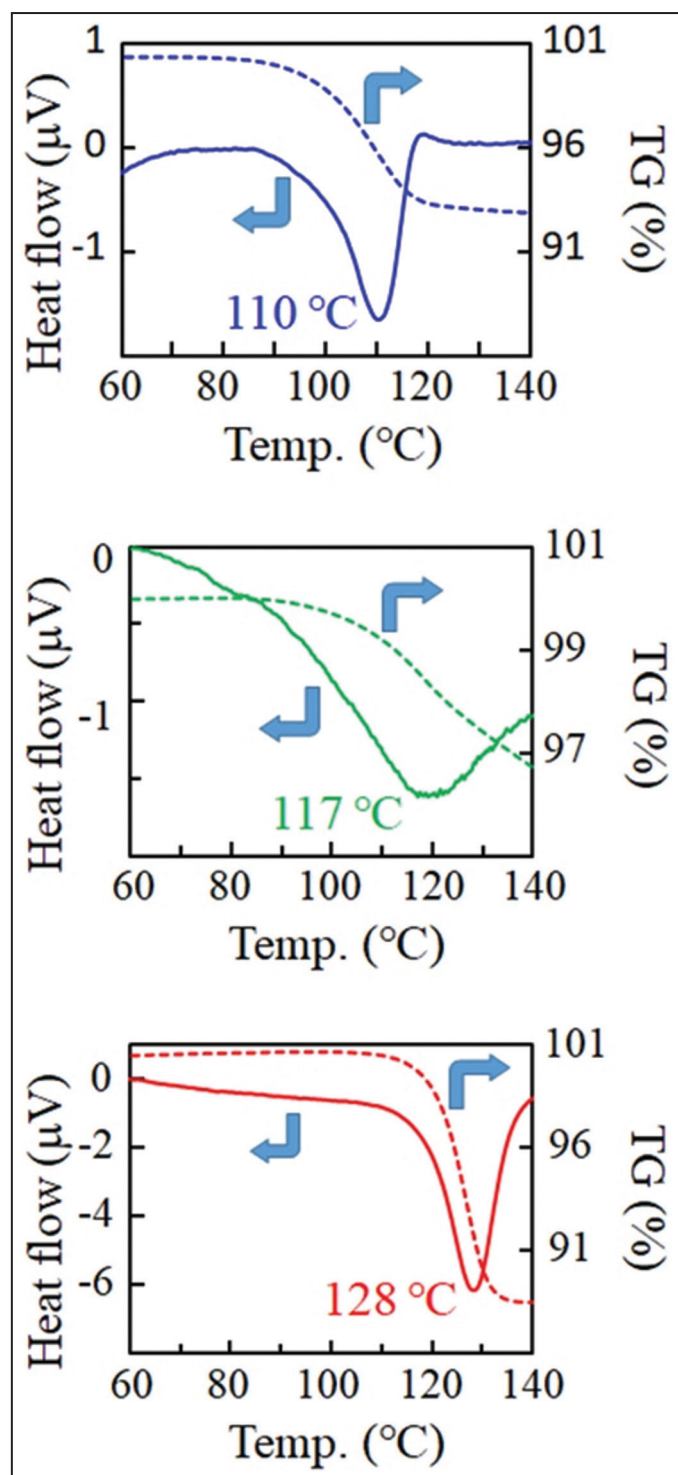## 5. CONCLUSION

HM, a spiro 3-aminoimidazolidine-2,4-dithione derivative, is a promising host molecule with high selectivity for planar aromatic guest molecules. Guest planar aromatic molecules were trapped through NH⋯π interaction forces between N–H of the amino group of **HM** and the π orbital of the guest molecule. A stronger NH⋯π interaction force led to a higher desorption temperature; that is, the hydrogen

Figure 4: Orbital diagrams of the HOMO and LUMO energy levels for the molecular compounds.
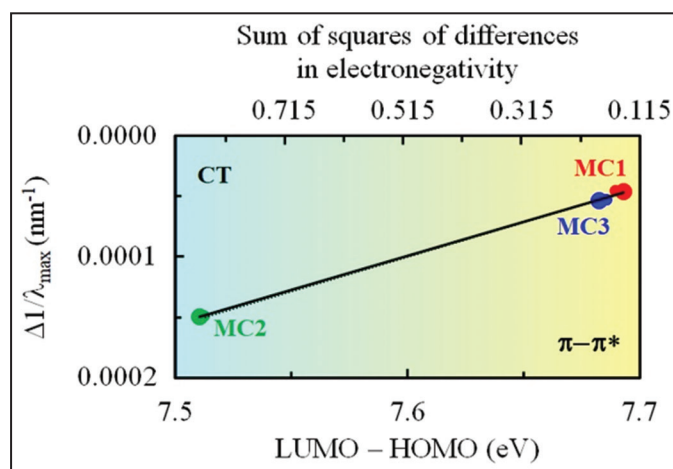
Figure 5: (Color online) Dependence of $\Delta 1/\lambda_{max}$ on the HOMO–LUMO gap and the sum of squares of differences in electronegativities.
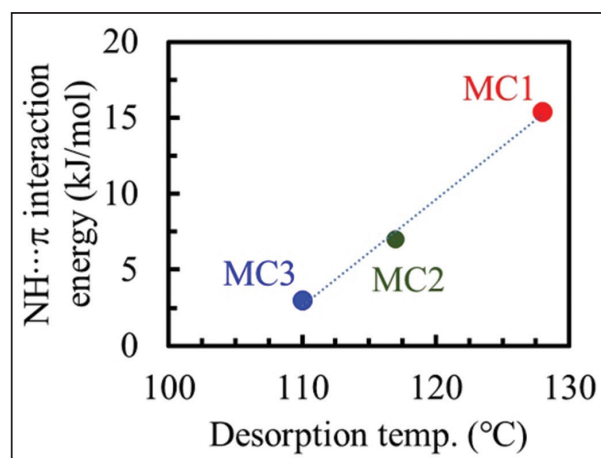
Figure 7: (Color online) Relationship between NH⋯π interaction energy and desorption temperature.

Figure 6: (Color online) TG-DTA profiles of the molecular compounds. From top to bottom: MC1, MC2, and MC3.

atom of the amino group of **HM** functions as a pin (or molecular tweezers without a fulcrum) to immobilize the guest molecule. Thus, **HM** can potentially be applied as a molecular tweezer, enabling the identification of trapped molecules through emission spectroscopy following guest molecule trapping.

7. REFERENCES

1. G. Yu, X. Chen, (2019) Host-guest chemistry in supramolecular theranostics, *Theranostics*, **9:** 3041-3074.

2. G. Yu, Y. Ma, C. Han, Y. Yao, G. Tang, Z. Mao, C. Gao, F. Huang, (2013) A sugar-functionalized amphiphilic pillar[5]arene: Synthesis, self-assembly in water, and application in bacterial cell agglutination, *Journal of American Chemical Society*, **135:** 10310-10313.

3. A. L. Horwich, G. W. Farr, W. A. Fenton, (2006) GroEL-GroES-mediated protein folding, *Chemical Reviews*, **106:** 1917-1930.

4. W. W. Grabow, L Jaeger, (2014) RNA self-assembly and RNA nanotechnology, *Accounts of Chemical Research*, **47:** 1871-1880.

5. A. Chworos, I. Severcan, A. Y. Koyfman, P. Weinkam, E. Oroudjev, H. G. Hansma, L. Jaeger, (2004) Complex shapes self-assembled from single-stranded DNA tiles, *Science*, **306:** 2068-2072.

6. C. W. Chen, H. W. Whitlock Jr., (1978) Molecular tweezers: A simple model of bifunctional intercalation, *Journal of American Chemical Society*, **100:** 4921-4922.

7. Y. Takazawa, T. Yamamoto, M. Suzuki, T. Sakata, (2018) Reversible formation of an inter-molecular compound comprising 3′-aminofluorene-9-spiro-5′-imidazolidine-2′,4′-dithione and benzene, *Heterocycles*, **96:** 2087-2095.

8. J. K. Savjani, A. K. Gajjar, (2011) Pharmaceutical importance and synthetic strategies for imidazolidine-2-thione and imidazole-2-thione derivatives, *Pakistan Journal of Biological Sciences*, **14:** 1076-1089.

9. S. C. Zimmerman, C. M. VanZyl, (1987) Rigid molecular tweezers: Synthesis, characterization, and complexation chemistry of a diacridine, *Journal of American Chemical Society*, **109:** 7894-7896.

10. S. C. Zimmerman, W. Wu, (1989) A rigid molecular tweezer with an active site carboxylic acid: An exceptionally efficient receptor for adenine in an organic solvent, *Journal of American Chemical Society*, **111:** 8054-8055.

11. S. C. Zimmerman, (1993) Supramolecular host–guest chemistry of heterocyclic V-shaped molecules, *Topics in Current Chemistry*, **165:** 71-102.

12. F. G. Klärner, B. Kahlert, (2003) Molecular tweezers and clips as synthetic receptors. Molecular recognition and dynamics in receptor−substrate complexes, *Accounts of Chemical Research*, **36:** 919-932.

13. Cambridge Crystallographic Data Centre. Crystal Data for 3'-aminofluorene-9-spiro-5'-imidazolidine-2',4'-dithione·1/2 Benzene Solvate. Cambridge: Cambridge Crystallographic Data Centre; 2018.

14. Cambridge Crystallographic Data Centre. Crystal data for 3'-aminofluorene-9-spiro-5'-imidazolidine-2',4'-dithione·1/2 Pyrrole Solvate. Cambridge: Cambridge Crystallographic Data Centre; 2019.

15. Cambridge Crystallographic Data Centre. Crystal Data for 3'-aminofluorene-9-spiro-5'-imidazolidine-2',4'-dithione·1/2 Thiophene Solvate. Cambridge: Cambridge Crystallographic Data Centre; 2019.

16. L. Pauling, (1932) The nature of the chemical bond. IV. The energy of single bonds and the relative electronegativity of atoms, *Journal of American Chemical Society*, **54:** 3570-3582.

17. R. T. Sanderson, (1983) Electronegativity and bond energy, *Journal of American Chemical Society*, **105:** 2259-2261.

18. R. T. Sanderson, (1988) Principles of electronegativity part II. Applications, *Journal of Chemical Education*, **65:** 227-231.

Bibliographical Sketch

Tomomi Sakata received the B.S. and M.S. degrees in Chemistry from Tohoku University, Japan, in 1989 and 1991, respectively. In 1991, he joined Nippon Telegraph and Telephone Corp., Japan, where he was engaged in research and development of optical devices. In 2016, he joined Josai University, Japan. He is currently working on developing the molecular tweezers. He is a member of the Japan Society of Applied Physics and the Institute of Electrical Engineers of Japan.

SUPPLEMENTARY DATA

Molecular compounds comprising HM and planar aromatic solvents

1. Molecular compound comprising HM and benzene (MC1)

HM was dissolved in benzene and was subsequently evaporated under reduced pressure. The resulting residue was then recrystallized by adding a 1:1 benzene/pentane solvent system. The obtained crystals were dried at 70 °C under a reduced pressure of 666 Pa for over 7.0 h to produce **MC1** [7]. Yield = 100%.

δ_H (in acetone-d_6) 10.038 (brs, 1H, NHC=S), 7.842 (d, 2H, J = 7.6 Hz, 1-H and 8-H), 7.484 (dt, 2H, J = 1.2 and 7.6 Hz, 2-H and 7-H), 7.363 (s, 3H, 1/2 benzene), 7.350 (dt, 2H, J = 1.2 and 7.6 Hz, 3-H and 6-H), 7.294 (d, 2H, J = 7.6 Hz, 4-H and 5-H), 6.140 (s, 1.6H, NH$_2$), and 6.116 (s, 0.4H, NHD) ppm.

δ_C (in acetone-d_6) 193.70 (C=S···DNH), 193.60 (C=S···HNH), 180.42 (NHC=SN), 144.88 (8a-C and 9a-C), 142.08 (4a-C and 5a-C), 131.02 (1-C and 8-C), 129.48 (2-C and 7-C), 129.09 (benzene), 124.73 (3-C and 6-C), 121.46 (4-C and 5-C) and 81.83 (9-C) ppm.

2. Molecular compound comprising HM and pyrrole (MC2)

HM was first dissolved in pyrrole, which was then evaporated under reduced pressure. The resulting residue was then left to stand without the addition of a low-solubility solvent. The obtained crystals were dried at 70 °C under a pressure of 500 Pa for over 4.0 h to yield **MC2**. Yield = 100%.

δ_H (in acetone-d_6) 10.006 (brs + brt, 1.5H, J = 60 Hz, NHC=S and 1/2 pyrrole 1-NH), 7.836 (dd, 2H, J = 1.2 and 7.6 Hz, 1-H and 8-H), 7.478 (dt, 2H, J = 1.2 and 7.6 Hz, 2-H and 7-H), 7.345 (dt, 2H, J = 1.2 and 7.6 Hz, 3-H and 6-H), 7.280 (ddd, 2H, J = 0.8, 1.2, and 7.6 Hz, 4-H and 5-H), 6.772 (dd, 1H, J = 2.4 and 4.4 Hz, pyrrole α-CH), 6.122 (s, 2H, NH$_2$), and 6.075 (dd, 1H, J = 2.4 and 4.4 Hz, pyrrole β-CH) ppm.

δ_C (in acetone-d_6) 193.58 (N-C=S), 180.45 (NHC=SN), 144.92 (8a-C and 9a-C), 142.11 (4a-C and 5a-C), 131.04 (1-C and 8-C), 129.49 (2-C and 7-C), 124.76 (3-C and 6-C), 121.48 (4-C and 5-C), 118.02 (pyrrole α-C), 108.11 (pyrrole β-C), and 81.87 (9-C) ppm.

δ_C (in DMSO-d_6) 193.97 (N-C=S), 180.06 (NHC=SN), 144.10 (8a-C and 9a-C), 141.21 (4a-C and 5a-C), 130.64 (1-C and 8-C), 129.18 (2-C and 7-C), 124.26 (3-C and 6-C), 121.32 (4-C and 5-C), 117.81 (pyrrole α-C), 107.57 (pyrrole β-C), and 81.14 (9-C) ppm.

3. Molecular compound comprising HM and thiophene (MC3)

HM was dissolved in thiophene, which was then evaporated under reduced pressure. The resulting residue was then recrystallized by adding *n*-hexane. The obtained crystals were dried at 70°C under a pressure of 500 Pa for over 4.0 h to afford **MC3**. Yield = 100%.

δ_H (in acetone-d_6) 10.013 (s, 1H, NHC=S), 7.830 (d, 2H, J = 8.0 Hz, 1-H and 8-H), *ca.* 7.47 (m, 3H, 2-H and 7-H and thiophene α-CH), 7.340 (t, 2H, J = 8.0 Hz, 3-H and 6-H), 7.283 (d, 2H, J = 8.0 Hz, 4-H and 5-H), 7.139 (dt, 1H, $J_{α,β}$ = 2.4 Hz and $J_{α,β'}$ = 0.8 Hz, thiophene β-CH), and 6.126 (s, 2H, NH$_2$) ppm.

δ_C (in acetone-d_6) 193.57 (N-C=S), 180.43 (NHC=SN), 144.88 (8a-C and 9a-C), 142.08 (4a-C and 5a-C), 131.03 (1-C and 8-C), 129.49 (2-C and 7-C), 127.68 (thiophene α-C), 125.98 (thiophene β-C), 124.73 (3-C and 6-C), 121.46 (4-C and 5-C), and 81.83 (9-C) ppm.

δ_C (in DMSO-d_6) 193.97 (N-C=S), 180.07 (NHC=SN), 144.09 (8a-C and 9a-C), 141.21 (4a-C and 5a-C), 130.64 (1-C and 8-C), 129.32 (2-C and 7-C), 129.19 (thiophene α-C), 124.80 (thiophene β-C), 124.26 (3-C and 6-C), 121.33 (4-C and 5-C), and 81.13 (9-C) ppm.